Probing the Nucleotide-Binding Site of *Escherichia coli* Succinyl-CoA Synthetase†

Michael A. Joyce,‡ Marie E. Fraser,‡,§ Edward R. Brownie,‡ Michael N. G. James,‡,§ William A. Bridger,|| and William T. Wolodko*,‡

Department of Biochemistry, University of Alberta, Edmonton, Alberta, Canada T6G 2H7, Medical Research Council of Canada Group in Protein Structure and Function, University of Alberta, Edmonton, Alberta, Canada T6G 2H7, and Office of the VP Research, University of Western Ontario, London, Ontario, Canada N6A 5B8

Received March 5, 1999; Revised Manuscript Received April 20, 1999

ABSTRACT: Succinyl-CoA synthetase (SCS) catalyzes the reversible interchange of purine nucleoside diphosphate, succinyl-CoA, and P_i with purine nucleoside triphosphate, succinate, and CoA via a phosphorylated histidine (H246α) intermediate. Two potential nucleotide-binding sites were predicted in the β-subunit, and have been differentiated by photoaffinity labeling with 8-N_3-ATP and by site-directed mutagenesis. It was demonstrated that 8-N_3-ATP is a suitable analogue for probing the nucleotide-binding site of SCS. Two tryptic peptides from the N-terminal domain of the β-subunit were labeled with 8-N_3-ATP. These corresponded to residues 107−119β and 121−146β, two regions lying along one side of an ATP-grasp fold. A mutant protein with changes on the opposite side of the fold (G53βV/R54βE) was unable to be phosphorylated using ATP or GTP, but could be phosphorylated by succinyl-CoA and P_i. A mutant protein designed to probe nucleotide specificity (P20βQ) had a $K_{m(app)}$ for GTP that was more than 5 times lower than that of wild-type SCS, whereas parameters for the other substrates remained unchanged. Mutations of residues in the C-terminal domain of the β-subunit designed to distrupt one loop of the Rossmann fold (I322βA, and R324βN/D326βA) had the greatest effect on the binding of succinate and CoA. They did not disrupt the phosphorylation of SCS with nucleotides. It was concluded that the nucleotide-binding site is located in the N-terminal domain of the β-subunit. This implies that there are two active sites ∼35 Å apart, and that the H246α loop moves between them during catalysis.

Succinyl-CoA synthetase (SCS)[1] catalyzes the substrate-level phosphorylation step of the citric acid cycle (for reviews, see refs *1* and *2*). SCS consists of two subunits designated α and β with approximate molecular masses of 31 and 42 kDa, respectively. The reaction catalyzed by SCS is thought to proceed via three partial reactions:

$$\text{E} + \text{succinyl-CoA} + \text{P}_\text{i} \rightleftharpoons \text{E·succinyl-PO}_3 + \text{CoA} \quad (1)$$

$$\text{E·succinyl-PO}_3 \rightleftharpoons \text{succinate} + \text{E-PO}_3 \quad (2)$$

$$\text{E-PO}_3 + \text{NDP} \rightleftharpoons \text{NTP} + \text{E} \quad (3)$$

where NDP and NTP are purine nucleoside di- and triphosphates, respectively, and E·succinyl-PO_3 represents a noncovalent association of SCS with succinyl phosphate. In the forward direction (as observed in the citric acid cycle), the result is the conversion of the high-energy thioester bond in succinyl-CoA to the high-energy phosphoanhydride bond in nucleoside triphosphate. In the reverse direction, the reaction catalyzed by SCS is thought to replenish the succinyl-CoA utilized during ketone body metabolism (*3*) and in the synthesis of heme (*4*). Investigation of SCS activity in various organisms and tissues, and the cloning of SCS from these sources, revealed that the nucleotide specificity of SCS differs; some are specific for ATP and some for GTP, and others (such as the enzyme from *Escherichia coli*) can accommodate either ATP or GTP (*5*−*11*). The equilibrium constant for the overall reaction is approximately 1 (*12*), so the direction of the reaction catalyzed by SCS depends on the local concentrations of nucleotides. Thus, SCS specific for ATP, functioning in the citric acid cycle, will readily respond to the energy changes of the cell because the ratio of ATP to ADP varies about 1 depending on the metabolic state of the cell. A GTP-specific enzyme would be expected to maintain the high level of succinyl-CoA required by CoA transferase during ketone body metabolism since the value of the GTP/GDP ratio in mammalian mitochondria has been estimated to be approximately 100 or higher (*3*, *6*). In support of this idea, a correlation has been shown to exist between the SCS activity that is specific for GTP and the utilization of ketone bodies (*7*, *8*, *12*).

The cloning and characterization of the ATP- and GTP-specific isozymes from pigeon breast and liver revealed that they consist of the same α-subunit but different β-subunits (*10*, *11*). This implies that the nucleotide specificity of SCS

† This work was funded by grants from the Medical Research Council of Canada (MRC Grants MT-2805 and GR-13303). M.A.J. was supported by a studentship from the Alberta Heritage Foundation for Medical Research.

* To whom correspondence should be addressed. Telephone: (780) 492-2419. Fax: (780) 492-0886. E-mail: wtwt@obi-wab.biochem.ualberta.ca.

‡ Department of Biochemistry, University of Alberta.

§ Medical Research Council of Canada Group in Protein Structure and Function, University of Alberta.

|| University of Western Ontario.

[1] Abbreviations: SCS, succinyl-CoA synthetase; 8-N_3-ATP, 8-azidoadenosine 5′-triphosphate; DD-ligase, D-alanine:D-alanine ligase. Specific amino acid residues in given subunits of SCS are designated by the one- or three-letter code followed by the residue number and either α or β to indicate the subunit.

10.1021/bi990527s CCC: $18.00
Published on Web 05/14/1999

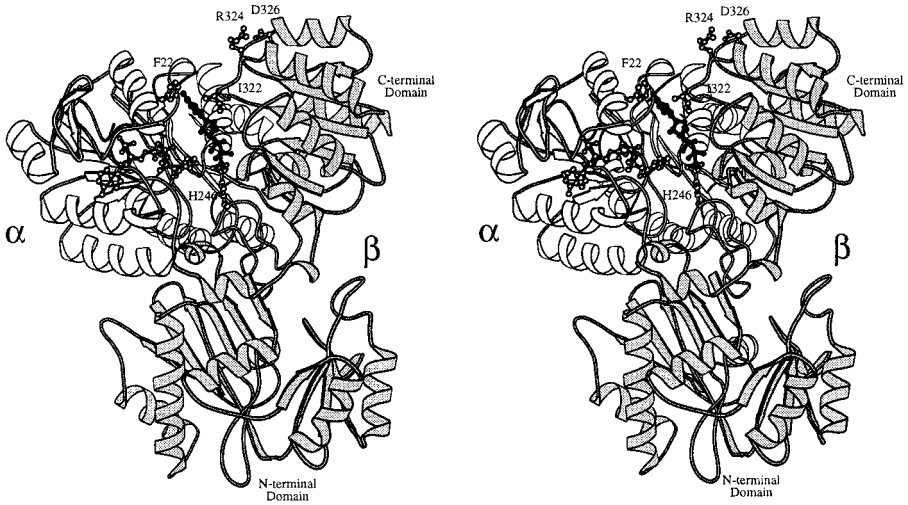

FIGURE 1: Stereo ribbon diagram of an $\alpha\beta$-dimer of SCS with an ATP molecule modeled into the C-terminal domain of the β-subunit. The α-subunit is shown in white, the β-subunit in gray, and the ATP molecule as a black ball-and-stick model. The active-site phosphohistidine, the bound CoA molecule, F22α, and the side chains of the residues that were mutated are displayed as white ball-and-stick models. This figure was constructed with the program MOLSCRIPT (*18*). Note that all of the stereo diagrams presented in this paper are divergent views.

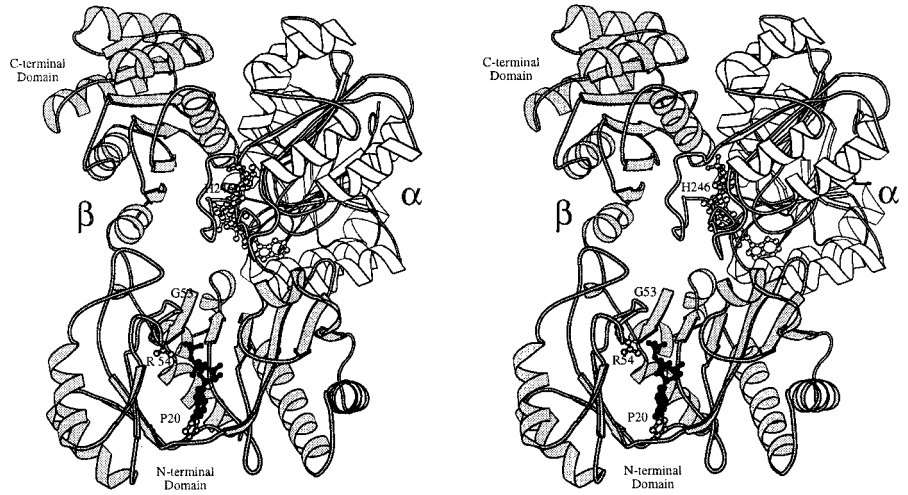

FIGURE 2: Stereo ribbon diagram of an $\alpha\beta$-dimer of SCS with an ADP molecule modeled into the N-terminal domain of the β-subunit. The α-subunit is shown in white, the β-subunit in gray, and the ADP molecule as a black ball-and-stick model. The active-site phosphohistidine, the bound CoA molecule, and the side chains of the residues that were mutated are displayed as white ball-and-stick models. This figure was constructed with the program MOLSCRIPT (*18*).

resides in the β-subunit. Although this implication contradicts an earlier study that suggested that the nucleotide-binding site was present in the α-subunit (*14*), it is consistent with the crystal structure of the *E. coli* enzyme. Both of the two nucleotide-binding (Rossmann) folds in the α-subunit are occupied, one by bound CoA and the other by the loop that contains the active-site phosphohistidine (*15*). However, there are two unoccupied potential nucleotide-binding sites in the β-subunit: a third Rossmann fold in the C-terminal domain (*15*) and the "ATP-grasp" fold in the N-terminal domain (*16*, *17*). The residues lining each of these sites are well-conserved among known amino acid sequences of SCS. Figures 1 and 2 show nucleotide modeled into each of these domains.

The location of each of these potential nucleotide-binding sites relative to the bound CoA and the active-site phosphohistidine would have direct and different consequences to our understanding of the catalytic mechanism of SCS. If the nucleoside triphosphate were bound in the C-terminal domain of the β-subunit (Figure 1), no substantial conformational change would be required for phosphorylation and/or dephosphorylation of the active-site histidine (partial reaction 3). If the nucleotide were bound in the N-terminal domain, then the active-site phosphohistidine is 35 Å away (Figure 2), and a major conformational change would therefore be required to bring the phosphohistidine into proximity with the nucleoside diphosphate (*17*).

Indirect support for a nucleotide-binding site being in the C-terminal domain of the β-subunit is 2-fold. First, previous studies have indicated that oxidized CoA disulfide binds to Cys 325β and inactivates SCS (*19*, *20*). We have found that the relative levels of protection of *E. coli* SCS from this modification afforded by ATP and GTP were consistent with the relative affinity of the enzyme for ATP and GTP (unpublished results). Second, ATP can be modeled into this site with the γ-phosphate of ATP superimposed on the phosphate of the phosphohistidine, and the adenosine ring positioned in a hydrophobic patch between the side chains of Ile 322β and Phe 22α (Figure 1). The loop containing Ile

322β may be anchored by an ion pair formed between Arg 324β and Asp 326β. In addition, these two residues are conserved among SCS enzymes that use ATP, whereas they are Asn and Ala, respectively, in SCS enzymes that are specific for GTP (*9*, *10*).

The prediction that a nucleotide-binding site resides in the N-terminal domain of the β-subunit of *E. coli* SCS is based on structural similarity between the ATP-grasp fold in the N-terminal domain and the nucleotide-binding fold found in glutathione synthetase (*21*) and D-alanine:D-alanine ligase (DD-ligase) (*22*). Many of the residues that contact the ADP in the nucleotide-binding folds of both glutathione synthetase and DD-ligase are also found in the N-terminal domain of the β-subunit (*17*). In addition, there is a sulfate ion bound in the N-terminal domain of the β-subunit in the crystal structure of *E. coli* SCS (*15*). This sulfate ion is 1.4 Å from the β-phosphate of the ADP in DD-ligase when the structure of DD-ligase is superimposed onto the N-terminal domain of the β-subunit (*17*). The amino acid sequence of the loop which binds this sulfate ion (51-AGGRGKXGGV-60) is conserved in all known SCS sequences.

The focus of this study was to determine the location of the nucleotide-binding site in *E. coli* SCS. Toward this end, 8-N_3-ATP was shown to be a suitable photoaffinity analogue for use with SCS, and it was used to label and to isolate peptides from the nucleotide-binding site. In parallel, site-directed mutagenesis studies of conserved residues within each of the potential nucleotide-binding sites were carried out. The possible roles of these residues in catalysis by SCS were evaluated by measuring the kinetic parameters of the mutant proteins and determining their ability to catalyze the partial phosphorylation reactions involving either nucleotide (partial reaction 3) or succinyl-CoA and P_i (partial reactions 1 and 2). In addition, mutation of a single residue in the N-terminal domain of the β-subunit altered the nucleotide specificity of *E. coli* SCS.

MATERIALS AND METHODS

Photolabeling of E. coli SCS by [α-^{32}P]-8-N_3-ATP. Wild-type *E. coli* SCS was overexpressed and purified according to the methods of Wolodko et al. (*15*, *23*). The ATP analogue, 8-N_3-ATP, was purchased from Sigma-Aldrich Canada Ltd. and [α-^{32}P]-8-N_3-ATP (2−10 Ci/mmol) from ICN Pharmaceuticals, Inc. For the saturation studies, 5 μg of SCS in 30 μL of a solution containing 50 mM KCl, 10 mM $MgCl_2$, 1 μM succinate, 0.12 μM CoA, and 50 mM MOPS (pH 7.4) was incubated for 15 s on ice with the appropriate concentration of [α-^{32}P]-8-N_3-ATP (0.1−0.3 Ci/mmol). The sample was then irradiated for 30 s using a hand-held UV6L Mineralight UV lamp (I = 360 μW/cm^2, λ = 254 nm) from a distance of 2 cm. The reaction was quenched by the addition of 1 μL of 0.25 M DTT. Next, 20 μL of SDS−PAGE loading buffer [2.5% (w/v) SDS, 1 mM 2-mercaptoethanol, 35% (v/v) glycerol, and 50 mM Tris-HCl (pH 6.6)] was added to the samples, which were then heated to 96 °C for 5 min prior to analysis by SDS−PAGE using a 12% (w/v) polyacrylamide gel (*24*). Phosphorimaging of the photolabeled SCS was carried out using a Fujix BAS 1000 phosphorimager. Exposure of the imaging plate was usually complete in 2−3 h. For inhibition of the photolabeling, 2 mM ATP or 3 mM GTP was included in the buffer during the photolabeling procedure. Apparent dissociation constants were determined by analysis of the labeling data using the program ENZYME KINETICS 1.11 (*25*).

Inactivation of SCS Activity by 8-N_3-ATP. The procedure was identical to the photolabeling procedure, except that 2.6 μg of SCS and nonradioactive 8-N_3-ATP were used. After quenching, 8 μL of each sample was assayed for SCS activity using a spectrophotometric assay that measures the extent of formation of the thioester bond of succinyl-CoA at 235 nm (*26*). To study the protection of SCS from inactivation by 8-N_3-ATP, 2 mM ATP or GTP was included in the buffer.

Determination of the $K_{m\ (app)}$ of SCS for 8-N_3-ATP. Kinetic reactions were conducted at 22 °C and started by the addition of 16.5 μg of SCS in 10 μL to 1 mL of a buffer containing 10 mM $MgCl_2$, 10 mM succinate, 100 μM CoA, 20 mM Tris-HCl (pH 7.4), and various concentrations of 8-N_3-ATP. The rate of formation of succinyl-CoA was monitored spectrophotometrically at 235 nm in duplicate at each concentration. The data were analyzed using the program SIGMA PLOT (*27*). The curve was fitted using the Hill equation, $v = V_{max}[S]^n/(K + [S]^n)$, where v is the velocity in micromoles per minute per milligram of SCS, V_{max} is the maximum velocity, [S] is the concentration of 8-N_3-ATP, K is a constant, and n is the Hill coefficient (*28*).

Photolabeling and Mass Spectrometry of SCS Subunits. Photolabeled SCS for mass spectrometry was prepared by irradiation of 30 μg of SCS in 400 μL of a buffer containing 50 mM KCl, 10 mM $MgCl_2$, 400 μM 8-N_3-ATP, and 50 mM MOPS (pH 7.4). Irradiation was carried out in a Southern New England Ultraviolet Co. RPM200 UV box (reactor λ = 350 nm) for 7 min at 4 °C. The α- and β-subunits were then separated by reverse phase HPLC using a Vydac 4.6 mm × 250 mm C_8 column on a Varian Vista series 5000 liquid chromatography system equipped with a Hewlett-Packard 1040 HPLC diode array detector. The mobile system consisted of 0.05% (v/v) trifluoroacetic acid in water (A) and 0.05% (v/v) trifluoroacetic acid in acetonitrile (B). The gradient for HPLC was 2% (v/v) B/min for 20 min followed by 0.5% (v/v) B/min for 40 min, at a flow rate of 1 mL/min. Fractions containing the separated subunits were analyzed using a VG Quatro electrospray mass spectrometer running in positive mode. The running buffer for the mass spectrometry was 50% (v/v) acetonitrile/water and 0.1% (v/v) trifluoroacetic acid.

Photolabeling of SCS by 8-N_3-ATP for Purification and Sequencing or Mass Spectrometry of Labeled Peptides. Photolabeled SCS was prepared by irradiation for 1 min of a total of 566 μg of SCS in 500 μL split into three similar aliquots containing 50 mM KCl, 10 mM $MgCl_2$, 400 μM [α-^{32}P]-8-N_3-ATP (30 Ci/mol), and 50 mM MOPS (pH 7.4) on ice. Irradiation (λ = 254 nm) was carried out from a distance of 2 cm. The aliquots were pooled, and the photolabeling was quenched by the addition of 3 μL of 1 M DTT. The labeled protein was separated from the free analogue in the reaction mixture on a 20 mL Sephadex G-50 column previously equilibrated with 20 mM Tris-HCl (pH 8.0). The labeled SCS eluted after the first 8 mL in a total volume of 3 mL. The labeled SCS was digested at 37 °C with 20 μg of modified sequencing grade trypsin (Boehringer Mannheim). After 12 h, the pH was adjusted to 6.0 with 3 μL of 11.6 M HCl, and 3 mL of 5 mM DTT and 100 mM ammonium acetate (pH 6.0) was added.

An Al^{3+} affinity column (Chelating Sepherose Fast Flow, purchased from Pharmacia Biotech Inc.) was prepared and chromatography performed according to the methods of Jayaram and Haley (*29*), except that 5 mL of Chelating Sepherose Fast Flow iminodiacetic acid was used, and the final elution step was carried out with 100 mM ammonium acetate and 10 mM sodium pyrophosphate (pH 8.0). The radiolabeled peptides eluted in the final step. Aliquots of 5 μL of each fraction were assayed for radioactivity using a Beckman LS 7800 liquid scintillation counter. The fractions containing radioactivity were pooled and further purified by reverse phase HPLC using the same column and HPLC system that was used for purification of the subunits. The HPLC gradient was isocratic for 30 min at 0% (v/v) B to allow elution of the flow through. This was followed by a gradient of 1% (v/v) B/min with a flow rate of 0.5 mL/min. Fractions of 0.5 mL were collected and aliquots assayed for radioactivity using a Beckman LS 7800 liquid scintillation counter. The peptides containing radioactivity were sequenced by Edman degradation with a Hewlett-Packard 1005A peptide sequencer. Mass spectrometry was performed using a VG Quatro electrospray mass spectrometer.

Construction of Site-Directed Mutants in the β-Subunit of SCS. Site-directed mutants were made in three steps using standard protocols for the PCR and overlap extension (*30*). The procedures that were used were essentially the same as those described by Ho et al. except that each primer was used at 0.25 μM. In all cases, the template for PCR was the plasmid pGS202 (*31*). The primers used for construction of the mutant plasmids were as follows: for P20βQ, the 5′-flanking primer 5′-TTTTACCTCTGGCGGTGATA-3′, the 3′-flanking primer 5′-GGGTTGATTTCGATCAACGC-3′, and the internal primers 5′-TACCAGCA**CAG**GTGGGT-TATG-3′ and complement; for G53βV/R54βE, the 5′-flanking primer 5′-TTTTACCTCTGGCGGTGATA-3′, the 3′-flanking primer 5′-GGGTTGATTTCGATCAACGC-3′, and the internal primers 5′-GTTCACGCTGGT**GTGGAG**GG-TAAAGCGGGC-3′ and complement; for I322βA, the 5′-flanking primer 5′-AAGAAACTCCGCACCTGATC-3′, the 3′-flanking primer 5′-CCTCCACTGCGGCAACAACC-3′, and the internal primers 5′-CTTCGGCGGT**GCC**GTTCGT-TGC-3′ and complement; and for R324βN/D326βA, the 5′-flanking primer 5′-AAGAAACTCCGCACCTGATC-3′, the 3′-flanking primer 5′-CCTCCACTGCGGCAACAACC-3′, and the internal primers 5′-GCGGTATCGTT**AAC**TGC-**GCT**CTGATCGCTG-3′ and complement. The nucleotides that are different from the wild-type sequence are shown in bold. The mutant fusion product for the mutations P20βQ and G53βV/R54βE and the vector pGS202 were digested with *Nde*I and *Bst*XI according to the manufacturer's specifications (New England Biolabs Inc.). The fragments were separated by electrophoresis in 1% (w/v) agarose in TAE buffer (*32*), excised, and purified using glass milk (*33*). Each mutant fragment was ligated to the vector fragment using T4 DNA ligase (15 °C for 8 h). The resulting mutant plasmids were then used to transform competent JM103 *E. coli* cells (*32*). The procedures for preparing the mutants I322βA and R324βN/D326βA were identical to those described above except that the restriction enzyme *Bpu*I 1102 was used instead of *Nde*I. The presence of mutations in all constructs was verified by DNA sequencing using an Applied Biosystems model 373 automated sequencer.

Expression and Purification of SCS Mutants. The SCS null strain TK3D18 (*34*) was transformed with the mutant plasmids. Mutant proteins were expressed and purified by methods described previously (*15*, *23*). All mutant proteins were produced in high yields (approximately 30−100 mg/L of culture). During purification, the elution profiles of all mutant proteins were identical to those of the wild-type enzyme. The mutant proteins were stored as suspensions in solutions containing 50% (w/v) $(NH_4)_2SO_4$ at 4 °C. Purified mutant proteins did not appear to have any changes in secondary structure compared to wild-type SCS as determined by UV CD from 180 to 255 nm (data not shown).

Steady-State Kinetic Analyses of SCS Mutants. For kinetic analyses, an aliquot of the appropriate $(NH_4)_2SO_4$ suspension was centrifuged (15000*g* for 30 min at 4 °C), and the pellet was dissolved in 500 μL of 50 mM KCl, 0.1 mM EDTA, and 50 mM Tris-HCl (pH 7.4). The resultant solution was clarified by centrifugation (15000*g* for 30 min at 4 °C) and dialyzed for 16 h with three changes of the same buffer at 4 °C. The concentration of the protein was determined spectrophotometrically using the extinction coefficient determined for wild-type SCS at 280 nm ($E^{1\%}_{1cm}$ = 5.0) (*35*). The concentrations of the nucleotides and CoA were determined using their standard extinction coefficients for a 1 cm path length (for ATP, E_{259nm} = 15.4 mM^{-1}, for GTP, E_{252nm} = 13.7 mM^{-1}, and for CoA, E_{260nm} = 14.6 mM^{-1}). The $K_{m\,(app)}$ and k_{cat} values in the direction of succinyl-CoA formation were measured at 22 °C. For each substrate, the initial velocity was measured at various substrate concentrations and at a constant concentration of the other substrates (where appropriate, 115 μM CoA, 60 mM succinate, or 510 μM ATP or GTP) in a total volume of 1 mL containing 50 mM KCl, 10 mM $MgCl_2$, and 50 mM Tris-HCl (pH 7.4). Initial rates were measured in duplicate at each substrate concentration, and the initial velocity data were analyzed using the ENZYME KINETICS 1.11 program for a Macintosh computer (*25*). All of the correlation coefficients for the straight lines in the Lineweaver−Burk plots were greater than 0.987. The k_{cat} values were obtained by division of the value for V_{max} by the molar concentration of active sites (i.e., per $\alpha\beta$-dimer) used in the experiments.

Phosphorylation Reactions Catalyzed by SCS Mutants. Phosphorylation of SCS by ATP or GTP (partial reaction 3) was carried out at 22 °C in 30 μL of a buffer containing 10 mM $MgCl_2$, 50 mM KCl, and 50 mM Tris-HCl (pH 7.4) with 1 mM [γ-^{32}P]ATP or [γ-^{32}P]GTP (approximately 0.3 Ci/mmol). Reactions were started by the addition of 5 μg of SCS in 2 μL, and the mixtures were incubated for various lengths of time before the addition of 15 μL of SDS−PAGE loading buffer to stop the reactions. Phosphorylation of SCS in the opposite direction by succinyl-CoA and P_i (partial reactions 1 and 2) was carried out in the same buffer except that [γ-^{32}P]ATP or [γ-^{32}P]GTP was replaced by 0.3 mM succinyl-CoA and 1 mM $^{32}P_i$ (approximately 0.3 Ci/mmol). The results were analyzed via SDS−PAGE [12% (w/v) polyacrylamide gels] and autoradiography, with the radioactively labeled bands quantified by phosphorimaging. Exposure of the image plate was complete in 1−2 h.

RESULTS

Several methods were used to determine if 8-N_3-ATP was an appropriate photoaffinity analogue of ATP for studies with

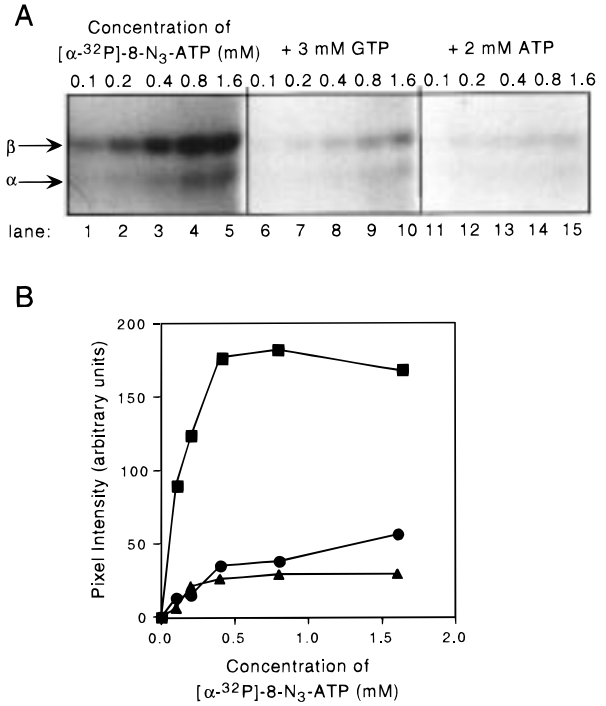

FIGURE 3: Saturation of photolabeling of SCS by [α-^{32}P]-8-N_3-ATP and prevention of photolabeling by ATP and GTP. (A) Autoradiogram of photolabeled SCS analyzed by SDS−PAGE. Lanes 1−5 contained SCS irradiated for 30 s in the presence, respectively, of 0.1, 0.2, 0.4, 0.8, and 1.6 mM [α-^{32}P]-8-N_3-ATP. In lanes 6−10, 3 mM GTP was included during irradiation. In lanes 11−15, 2 mM ATP was included during irradiation. (B) Quantitation of the incorporation of [α-^{32}P]-8-N_3-ATP into the β-subunit of SCS by phosphorimagery: (■) with 8-N_3-ATP alone (corresponding to lanes 1−5 in panel A), (●) with 8-N_3-ATP and 3 mM GTP (corresponding to lanes 6−10), and (▲) with 8-N_3-ATP and 2 mM ATP (corresponding to lanes 11−15).

SCS. It was shown that 8-N_3-ATP labels SCS in a saturable manner that was coincident with the inactivation of SCS. It was also shown that 8-N_3-ATP was a substrate for SCS and, upon irradiation, labeled the β-subunit with a stoichiometry of one 8-N_3-ATP per β-subunit.

Photolabeling of SCS by 8-N_3-ATP. Irradiation of SCS for 30 s resulted in saturable labeling of SCS with [α ^{32}P]-8-N_3-ATP (Figure 3). Control samples of SCS were not labeled by [α-^{32}P]-8-N_3-ATP when incubations were carried out in the dark, or when the irradiation step was carried out prior to the addition of SCS (data not shown). As is evident from the autoradiograms, photolabeling occurred predominantly in the β-subunit (Figure 3A). Some labeling of the α-subunit was observed at the highest analogue concentrations that were tested ($\lambda = 254$ nm) and may have resulted from low affinity for nucleotide leading to nonspecific labeling (*36*). Labeling was inhibited by the addition of 2 mM ATP or 3 mM GTP (Figure 3), indicating that the binding of 8-N_3-ATP was specific for the nucleotide-binding site of SCS. The extent of labeling by [α-^{32}P]-8-N_3-ATP was dependent on the concentration of the analogue, and saturation of labeling of the β-subunit was observed at approximately 0.5 mM (Figure 3B). From a double-reciprocal plot of the labeling data, the value of $K_{d(app)}$ for 8-N_3-ATP in the presence of other substrates was estimated to be 54 μM. A better estimate of K_d for 8-N_3-ATP would require that the analogue not be altered by the enzyme. Although the labeling

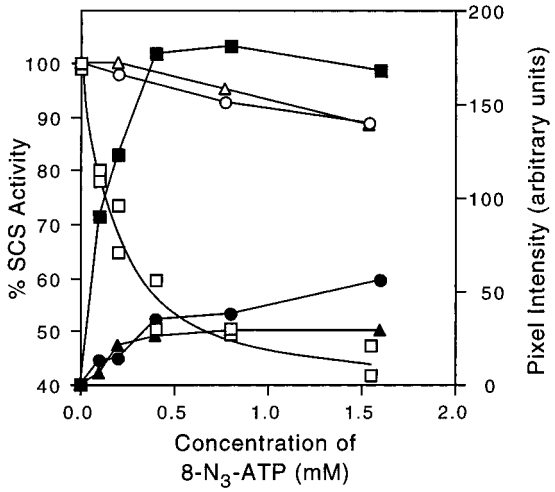

FIGURE 4: Correlation of the extent of photolabeling of the β-subunit with the extent of inactivation of SCS when irradiation is carried out for 30 s. White symbols represent data from measurements of the SCS activity after irradiation in the presence of various concentrations of 8-N_3-ATP. Black symbols represent data from photoincorporation of [α-^{32}P]-8-N_3-ATP into the β-subunit as assayed by phosphorimagery of SDS−PAGE gels: (□ and ■) SCS irradiated in the presence of 8-N_3-ATP alone, (△ and ▲) irradiation in the presence of 8-N_3-ATP and 2 mM ATP, and (○ and ●) irradiation in the presence of 8-N_3-ATP and 3 mM GTP.

was carried out on ice to preclude catalysis by the enzyme, there may still have been some turnover of the analogue. The value of the $K_{d(app)}$ derived from labeling experiments carried out in the absence of succinate and CoA was 90 μM. These $K_{d(app)}$ values for 8-N_3-ATP were consistent with the $K_{m\ (app)}$ value of 70 μM (this study) and the $K_{d(app)}$ value of 68 μM (*37*) determined at 25 °C for ATP and ADP, respectively, and were therefore considered reasonable.

Is 8-N_3-ATP a Substrate for SCS? To determine if 8-N_3-ATP behaves as a substrate for SCS, in a manner consistent with the labeling, a kinetic analysis of the associated enzymatic activity was performed. Initial rates of formation of succinyl-CoA were measured in solutions containing various concentrations of 8-N_3-ATP and saturating concentrations of succinate and CoA. The plot of velocity of SCS activity versus concentration of 8-N_3-ATP was sigmoidal, and a Hill plot was used to determine the kinetic constants. The value of $K_{0.5V_{max}}$ extrapolated from the graph was 210 μM, the V_{max} 0.074 μmol min^{-1} mg^{-1}, and the Hill coefficient 1.7. This value for $K_{0.5V_{max}}$ is comparable to the value of 90 μM for $K_{d(app)}$ obtained from the labeling experiments, and consistent with 8-N_3-ATP acting as a substrate.

Inactivation of SCS by 8-N_3-ATP. Irradiation of SCS in the presence of 8-N_3-ATP resulted in the loss of SCS activity (Figure 4). This inactivation was concentration-dependent, and the activity of SCS was inversely related to the degree of photoincorporation of [α-^{32}P]-8-N_3-ATP into the β-subunit of SCS. The presence of ATP or GTP protected SCS from both photoincorporation and inactivation. When samples were irradiated for 30 s, inhibition to 45% of the initial activity was observed at the highest analogue concentrations that were tested (Figure 4). Irradiation for longer lengths of time (for example, 5 min) in the presence of 8-N_3-ATP resulted in greater labeling and total inactivation of SCS, and both were prevented by the addition of ATP or GTP (data not shown).

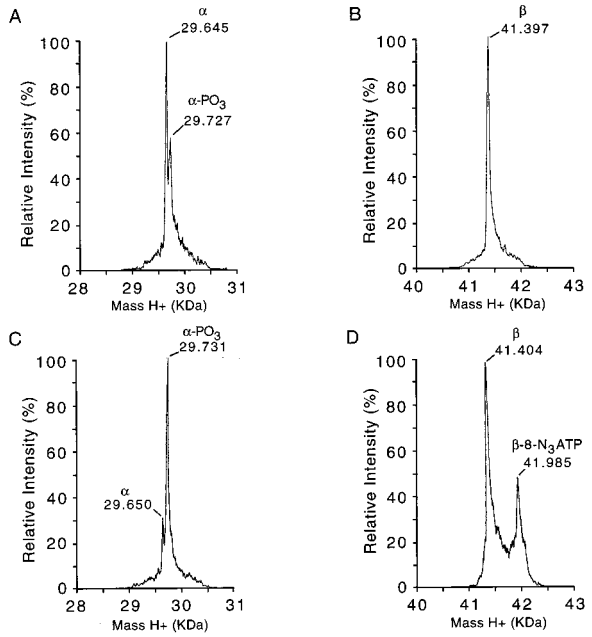

FIGURE 5: Electrospray mass spectra of the subunits of SCS. SCS was irradiated either in the absence (A and B) or in the presence (C and D) of 8-N_3-ATP, and the subunits were separated by reverse phase HPLC, followed by mass spectrometry of the isolated subunits (see Materials and Methods for specific details). Data for the α-subunit are shown in panels A and C, and data for the *β*-subunit are shown in panels B and D.

Mass Spectrometry of SCS Subunits Labeled by 8-N_3-ATP. To determine the stoichiometry of labeling, electrospray mass spectrometry was performed on photolabeled α- and *β*-subunits separated by HPLC. The results are shown in Figure 5. When irradiation at 350 nm was carried out in the absence of 8-N_3-ATP, there were two species present in HPLC fractions containing the α-subunit and one in the fractions containing the *β*-subunit (Figure 5A,B). In the case of the α-subunit, the major species had a mass of 29 645 Da, corresponding to the predicted mass of 29 647 Da for the purified α-subunit that lacks the N-terminal methionine (*1*, *38*). The major species was 82 Da smaller than the minor species (Figure 5A), corresponding to the mass of H_2PO_3 (81 Da) and indicating that the major portion of the population of the α-subunit was dephosphorylated. In the case of the *β*-subunit (Figure 5B), the only species present had a mass of 41 397 Da, that of the unmodified *β*-subunit (41 394 Da). When 400 *μ*M 8-N_3-ATP was added to the reaction mixture, in the case of the α-subunit, again two species were observed (Figure 5C); however, the species with a higher mass was now prominent. This indicated that the α-subunit was phosphorylated during the course of the labeling reaction, in keeping with our conclusion that 8-N_3-ATP was acting as a substrate. Two species were also observed in HLPC fractions containing the *β*-subunit when SCS was irradiated in the presence of 8-N_3-ATP (Figure 5D). The smaller of the two had a mass of 41 404 Da, and the larger species had a mass of 41 985 Da. The difference between the two masses corresponds to one 8-N_3-ATP (520 Da) and an extra 61 Da. The extra mass may be due to one Mg^{2+} ion (24 Da) and one K^+ ion (39 Da) chelating to the 8-N_3-ATP, or it may be due to two molecules of NO (60 Da). The NO molecules may have arisen from the liberation of $N_2^{\bullet}$ during irradiation, which could have reacted with oxygen, and subsequently attached to the protein. The reaction of oxygen with nitrophenyl azides has been shown to occur during low-power irradiation of these compounds (*39*). When irradiation was carried out in the presence of a saturating concentration of 8-N_3-ATP (800 *μ*M), the only difference observed was an increase in the amount of the *β*-subunit species labeled with one 8-N_3-ATP. There was no evidence of a *β*-subunit species that had been modified by two or more molecules of 8-N_3-ATP, nor was there evidence of an α-subunit species that had been modified by even one 8-N_3-ATP. These observations support our earlier interpretation that under the harsher conditions of the initial experiments (Figure 3), the labeling of the α-subunit was nonspecific. Note that irradiation at 350 nm gave rise to a limited number of products and therefore an easily interpretable mass spectrum, whereas irradiation at 254 nm led to the complex production of multiple products.

Isolation of 8-N_3-ATP-Photolabeled Peptides from SCS. To determine the location of the 8-N_3-ATP-binding site, peptide fragments of photolabeled SCS were generated by tryptic digestion, purified, and then analyzed by amino acid sequencing and mass spectrometry. Photolabeling of SCS was carried out by irradiation of SCS at 254 nm for 1 min in the presence of 400 *μ*M [α-^{32}P]-8-N_3-ATP. As a compromise, the harsher wavelength of 254 nm was used to maximize the yield of labeled peptides, and the midrange concentration of 400 *μ*M analogue to minimize nonspecific labeling. Typically, 0.42 mol of [α-^{32}P]-8-N_3-ATP was incorporated per mole of SCS. Following digestion, labeled peptides were separated from unlabeled peptides by Al^{3+} affinity chromatography (*29*). After the loaded column had been washed with buffers containing low salt, high salt, and urea to disrupt nonspecific electrostatic and hydrophobic interactions that may cause unlabeled peptides to be retained on the column, 85% of the radioactivity initially bound to the column remained bound (Figure 6A). No radioactively labeled peptides were found in the salt and urea washes by subsequent reverse phase HPLC analyses. The bound radioactivity was eluted from the affinity column using 10 mM pyrophosphate, and pooled. Subsequent reverse phase HPLC analysis of these pooled fractions revealed three major peaks with radioactivity. The first peak, containing most of the total radioactivity, appeared in the HPLC flow through fractions which eluted before the beginning of the chromatogram (data not shown). No peptide was found in these fractions. Similar losses of radioactive label have been observed in other studies in which azido analogues have been used (*29*, *40*). The other two peak fractions containing significant amounts of radioactivity eluted at 37 and 42 min, respectively (Figure 6B). Although the yields of the purified peptides were low (approximately 20 pmol), these peptides displayed a A_{210nm}/A_{255nm} ratio of close to 1, consistent with the presence of the aromatic adenine moiety. Edman degradation analysis of the peptide in the peak that eluted at 42 min gave the following sequence: VVFMASTEGGVEAEKVAEETPHLLHK. This corresponds to a tryptic peptide from amino acid residue 121 to 146 of the *β*-subunit of SCS. The mass of the material in this fraction was 3368 Da as determined by mass spectrometry. This corresponds to the mass of the peptide (2850.5 Da) plus the mass of the analogue (520 Da). The material in the peak that eluted at 37 min was also subjected to mass spectrometry and revealed two major species with masses

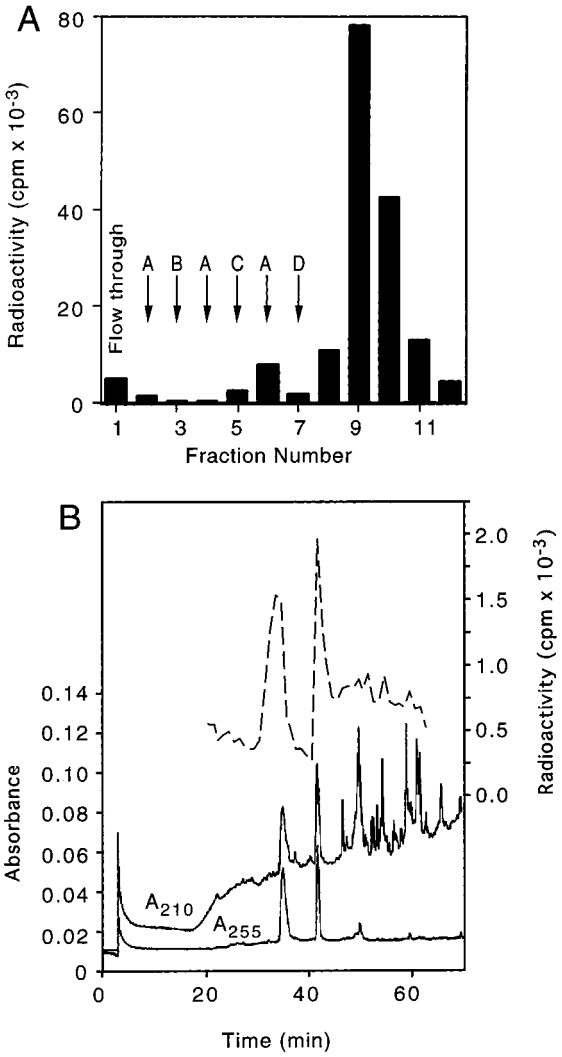

FIGURE 6: Purification of photolabeled peptides of SCS by Al^{3+} affinity chromatography (A) and reverse phase HPLC (B). (A) The Al^{3+} affinity column was loaded with the tryptic digest of photolabeled SCS and washed sequentially with the indicated solutions: A [5 mM DTT and 100 mM $(NH_4)_2SO_4$ (pH 6.0)], B [5 mM DTT, 0.5 M NaCl, and 100 mM $(NH_4)_2SO_4$ (pH 6.0)], C [5 mM DTT, 8 M urea, and 100 mM $(NH_4)_2SO_4$ (pH 6.0)], and D [5 mM DTT, 10 mM pyrophosphate, and 100 mM $(NH_4)_2SO_4$ (pH 8.0)]. The ^{32}P levels were determined as described in Materials and Methods. (B) Separations were carried out with a linear gradient of 1% (v/v) acetonitrile/TFA per minute with a flow rate of 0.5 mL/min as described in Materials and Methods. The solid lines represent the absorbance at 210 or 255 nm, and the dashed line represents the radioactivity associated with 0.5 mL fractions as assayed by liquid scintillation counting.

of 1466 and 520 Da. These correspond to a tryptic peptide from amino acid residue 107 to 119 of the β-subunit and a detached analogue. Obviously, the ionization of the labeled peptide during mass spectroscopy had caused the photo-insertion bond to break. Unfortunately, we were unable to sequence this peptide. Nevertheless, both of these results are consistent with a nucleotide-binding site being located in the N-terminal domain of the β-subunit.

Site-Directed Mutagenesis of Residues in the N-Terminal Domain of the β-Subunit. We chose to mutate residues Gly 53β and Arg 54β in the N-terminal domain. These residues are present in the conserved A51β−V60β loop; Gly 53β has hydrogen bonding and Arg 54β ionic interactions with the sulfate ion in the crystal structure of *E. coli* SCS (*17*). It was reasoned that mutation of these residues would disrupt their interactions with the terminal phosphates of the nucleotide if nucleotide were bound at this site. The location of the mutated residues in relation to a molecule of ADP modeled into the N-terminal domain is shown in Figure 2.

The kinetic parameters for the G53βV/R54βE double mutant were determined by steady-state analysis of initial rates of succinyl-CoA formation, and the results are summarized in Table 1. Kinetic analysis of the G53βV/R54βE mutant protein revealed one major difference when compared to wild-type SCS, an approximate 300-fold decrease in k_{cat} with either ATP or GTP (Table 1). The values of $K_{m\ (app)}$ for the other substrates remained comparable to those of the wild-type enzyme.

To determine which partial reactions for phosphorylation of SCS were impaired by these mutations, single-turnover experiments were performed with [γ-^{32}P]ATP, [γ-^{32}P]GTP (partial reaction 3), or succinyl-CoA and $^{32}P_i$ (partial reactions 1 and 2). The α-subunit of the G53βV/R54βE mutant protein was not phosphorylated by either [γ-^{32}P]ATP or [γ-^{32}P]GTP (panels A and B of Figure 7, respectively), but was fully phosphorylated by succinyl-CoA and $^{32}P_i$ (Figure 7C). These results are consistent with Gly 53 and/or Arg 54 of the β-subunit playing a role during transfer of the γ-phosphate of ATP or GTP (bound in the N-terminal domain) to the active-site histidine of the α-subunit.

Two residues that may be involved in determining the nucleotide specificity of SCS were predicted from the superposition of the N-terminal domain of *E. coli* SCS on DD-ligase (*17*), in combination with sequence comparisons of SCS enzymes with different nucleotide specificities. One residue, Glu 99β of *E. coli* SCS, superimposes with Glu 180 of DD-ligase, the residue that makes a hydrogen bond with the amino group at the 6 position of the adenine ring of ADP. GTP has a keto group at the 6 position of the guanine ring, and SCS specific for GTP contains an alanine residue at the corresponding location (*9*, *10*). The second residue that can provide specificity is located at position 20β. The GTP-specific enzymes have a glutamine residue that we postulate forms a hydrogen bond with O6 of GTP. However, *E. coli* SCS and the ATP-specific enzymes (*10*) have a proline residue at this position. To investigate one of these possible determinants of nucleotide specificity, we chose to mutate the proline residue to glutamine, reasoning that the change should increase the affinity of the *E. coli* enzyme for GTP.

The mutant P20βQ was prepared and analyzed in a manner similar to that of the G53βV/R54βE mutant. The results of the kinetic analyses (listed in Table 1) revealed that while the $K_{m(app)}$ for ATP had increased slightly, the value for GTP had decreased more than 5-fold. Furthermore, a comparison of the $k_{cat}/K_{m(app)}$ ratios for ATP and GTP clearly demonstrated that GTP was a better substrate than ATP for the P20βQ mutant, which was opposite from that observed for wild-type SCS. This result supports the hypothesis that Gln 20β forms a hydrogen bond with O6 of GTP in the mutant protein, and that this residue is involved in determining the nucleotide specificity of SCS.

Site-Directed Mutagenesis of Residues in the C-Terminal Domain of the β-Subunit. Given that a large conformational change in SCS would be required if nucleotide was bound in the N-terminal domain of the β-subunit, it was important

Table 1: Kinetic Parameters of Wild-Type and Mutant SCS Proteins[a]

protein	succinate $K_{m(app)}$ (mM)	CoA $K_{m(app)}$ (μM)	ATP $K_{m(app)}$ (μM)	ATP k_{cat} (min^{-1})	ATP $k_{cat}/K_{m(app)}$ ($\times 10^{-3}$ M^{-1} s^{-1})	GTP $K_{m(app)}$ (μM)	GTP k_{cat} (min^{-1})	GTP $k_{cat}/K_{m(app)}$ ($\times 10^{-3}$ M^{-1} s^{-1})
wild-type	0.25	4.0	70	2684	639	394	1471	62.2
mutations in the N-terminal domain of the β-subunit								
P20βQ	1.6	3.7	131	1065	135	73	807	184
G53βV/R54βE	1.0	4.3	126	7.8	1.03	354	5.0	0.235
mutations in the C-terminal domain of the β-subunit								
I322βA	14	17	90	533	98.7	239	521	36.3
R324βN/D326βA	3.6	13	95	3124	548	374[b]	ND[c]	–

[a] Measured by following the production of succinyl-CoA spectrophotometrically at 235 nm. See Materials and Methods for specific details. [b] An estimate based on measurements using a single GTP concentration (300 μM) which is comparable to the $K_{m(app)}$ value for the wild-type enzyme. [c] Not determined.

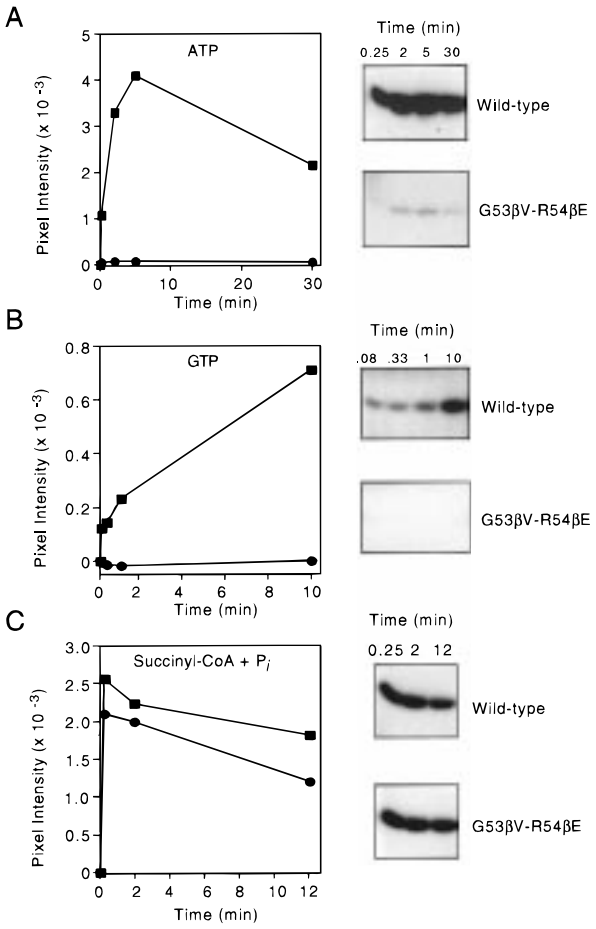

FIGURE 7: Time course of the phosphorylation reactions catalyzed by wild-type SCS and by one mutant of SCS with changes in the N-terminal domain of the β-subunit. Wild-type and mutant SCS were incubated in the presence of (A) [γ-^{32}P]ATP, (B) [γ-^{32}P]GTP, or (C) succinyl-CoA and $^{32}P_i$. Samples were taken at various times, and the subunits were analyzed by SDS−PAGE. Note that only the α-subunit [containing the active-site histidine (H246)] could be phosphorylated. The autoradiograms of the relevant portions of the gels are shown on the right. The results of subsequent phosphorimagery are plotted on the left: (■) wild-type SCS and (●) the protein with the double mutation G53βV/R54βE.

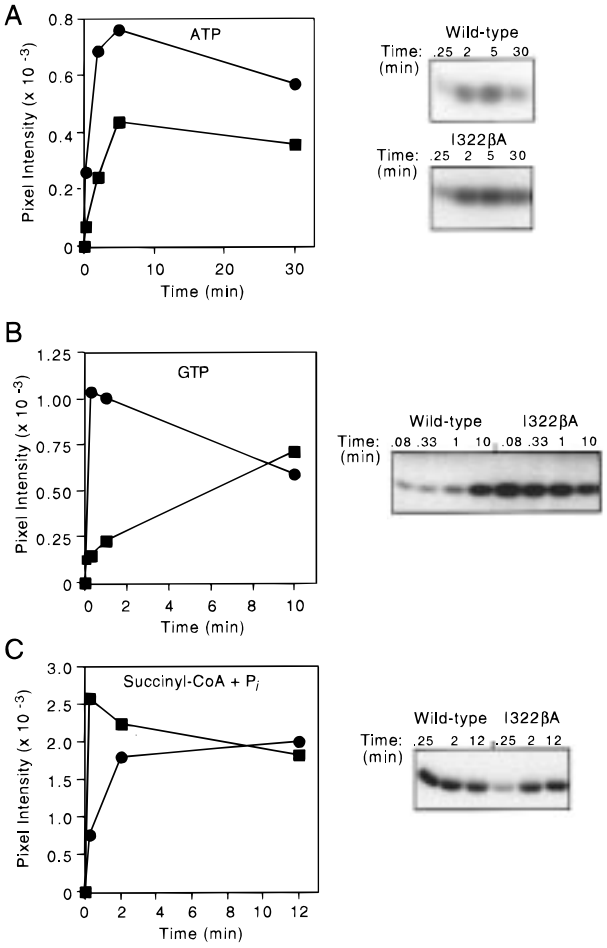

FIGURE 8: Time course of the phosphorylation reactions catalyzed by wild-type SCS and by one mutant of SCS with changes in the C-terminal domain of the β-subunit. Wild-type and mutant SCS were incubated in the presence of (A) [γ-^{32}P]ATP, (B) [γ-^{32}P]GTP, or (C) succinyl-CoA and $^{32}P_i$. Samples were taken at various times, and the subunits were analyzed by SDS−PAGE. Note that only the α-subunit [containing the active-site histidine (H246)] could be phosphorylated. The autoradiograms of the relevant portions of the gels are shown on the right. The results of subsequent phosphorimagery are plotted on the left: (■) wild-type SCS and (●) the protein with the mutation I322βA.

to consider the evidence from modeling and separate studies using oxidized CoA disulfide that indicated that the Rossmann fold in the C-terminal domain of the β-subunit may also bind nucleotide. In this light, we wished to investigate the role of three conserved residues in the C-terminal domain of the β-subunit implicated by modeling studies. Therefore, we chose to mutate residues Ile 322β, Arg 324β, and Asp 326β to probe this potential site (Figure 1). It was reasoned that mutation of these residues would disrupt a loop in the Rossmann fold, and thus disrupt any putative nucleotide binding in the C-terminal domain of the β-subunit.

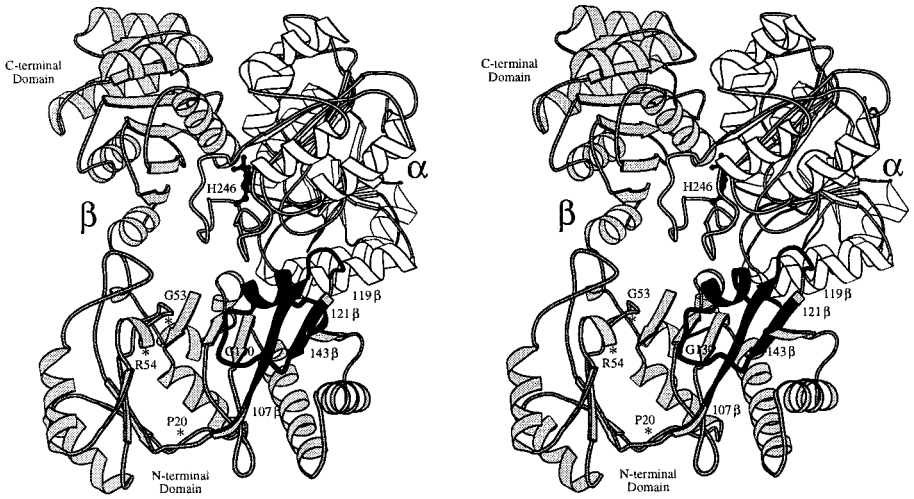

FIGURE 9: Stereo ribbon diagram of one αβ-dimer of *E. coli* SCS. The α-subunit is shown in white and the β-subunit in gray. The active-site phosphohistidine (H246α) is shown as a black ball-and-stick model. The two peptide segments in the β-subunit (residues 107−119 and 121−143) that were labeled with [α-^{32}P]-8-N_3-ATP and isolated by tryptic digestion are also shown in black. Residues 107β and 130β within these peptide segments are closest to the proposed site of nucleotide binding. The position of each residue mutated in the N-terminal domain of the β-subunit is marked by an asterisk (*), and labeled accordingly. This figure was constructed with the program MOLSCRIPT (*18*).

The mutant proteins were prepared and analyzed in a manner similar to that described earlier. Steady-state kinetic analyses of the proteins with mutations in the C-terminal domain of the β-subunit revealed few differences in kinetic parameters when compared to those of wild-type SCS (Table 1). The major changes observed were increases in the values of $K_{m(app)}$ for succinate and CoA. For example, the I322βA mutant protein exhibited an approximately 56-fold increase in the value of $K_{m(app)}$ for succinate compared to that of wild-type SCS. Together, these results implied that Ile 322β, Arg 324β, and Asp 326β are proximal to the succinate- and CoA-binding sites.

To determine which of the phosphorylation reactions may be impaired by these mutations, single-turnover experiments were performed with [γ-^{32}P]ATP or [γ-^{32}P]GTP (partial reaction 3), or succinyl-CoA and $^{32}P_i$ (partial reactions 1 and 2). The rate of phosphorylation of mutant proteins by [γ-^{32}P]-ATP (Figure 8A) or [γ-^{32}P]GTP (Figure 8B) was equal to or faster than that of wild-type SCS. The rate of phosphorylation by succinyl-CoA and $^{32}P_i$ (partial reactions 1 and 2) had decreased when compared to that of wild-type SCS (Figure 8C). These results were the reciprocal of those observed for the mutations tested in the N-terminal domain of the β-subunit, and consistent with the conclusion that Ile 322β, Arg 324β, and Asp 326β are not involved with binding nucleotide.

DISCUSSION

This study was undertaken to differentiate between two possible locations of the nucleotide-binding site in the β-subunit of *E. coli* SCS. We conclude that the nucleotide binds in the ATP-grasp fold of the N-terminal domain and not in the Rossmann fold of the C-terminal domain. Our results with the C-terminal domain mutants are consistent with previous work in which Cys 325β, a residue also in the Rossmann fold, was mutated to Gly with no affect on the overall enzymatic activity (*20*). Binding of the nucleotide in the N-terminal domain requires that the catalytic His 246α interact alternately at two sites, site I where CoA and, presumably, succinate bind and site II where the nucleotide binds. NMR spectroscopy studies produced evidence for a "flip" between two conformations of the phosphorylated histidine (*41*). His 246α is part of a loop that we postulate swings to shuttle the histidine residue between the two sites during each catalytic cycle.

The specific mutations that we made in the C-terminal domain affected the partial reactions involving CoA and succinate, but not nucleotide. We would interpret from the relative increase in the kinetic parameters observed for these two substrates (Table 1) that succinate and CoA are poorer substrates for the mutants than for the wild-type enzyme. It was thus not surprising that the mutants were more slowly phosphorylated by succinyl-CoA and P_i (Figure 8). Furthermore, we think that disruption of the succinate and CoA binding would indirectly affect the movement of the phosphohistidine loop. If the conformation with the loop bound to the α-subunit (as seen in the crystal structure) were destabilized, the rate of phosphorylation by succinyl-CoA and P_i at site I would be reduced while the rate of phosphorylation by the nucleotide at site II would be increased. These are the effects observed with the Ile 322β mutant (Figure 8).

The results from the studies with 8-N_3-ATP showed that it was a suitable analogue for probing the nucleotide-binding site of SCS: 8-N_3-ATP is a substrate with comparable kinetic parameters, its binding is saturable, the activity of SCS decreases reciprocally with labeling, and the addition of either ATP or GTP competitively precludes labeling. However, the velocity versus substrate plots with 8-N_3-ATP were observed to be sigmoidal. This could be indicative of a cooperative mechanism, but such a mechanism with ATP has not been observed for SCS (*42*). Furthermore, by mass spectrometry we observed only one molecule of 8-N_3-ATP bound per β-subunit when the concentration of 8-N_3-ATP was 2−4 times greater than $K_{0.5V_{max}}$. A sigmoidal curve can also be caused by the presence of multiple reaction pathways (*43*, *44*), and there is evidence that minor pathways exist for SCS (*37*, *45*). The comparatively low k_{cat} observed for 8-N_3-ATP

may allow minor pathways to become significant and compete for the substrate, hence the sigmoidal curve.

Photolabeling with 8-N_3-ATP marked two tryptic peptides that are part of the nucleotide-binding site in the N-terminal domain of the β-subunit (Figure 9). In the crystal structure, residues 121−146β include a loop that corresponds to the one that closes over the nucleotide-binding site in DD-ligase. Residues 107−119β lie under this loop, and residue Glu 107β has a counterpart in DD-ligase that forms hydrogen bonds with the ribose hydroxyl groups of ADP. On the basis of the structure of ADP in complex with DD-ligase, the 8-N_3-ATP analogue could not bind in the anti conformation without the azido group clashing with the ribose. Rotation of the adenine ring toward the syn conformation would allow the analogue to fit, albeit poorly (recall $K_{0.5V_{max}} = 210$ μM). Moreover, such a rotation would present the azido group to residue Glu 107β and toward residue Gly 130β of the loop (the closest residues within the two peptide segments), thus facilitating the observed photolabeling. The preferred conformation of ATP analogues with substituents at the 8-position is syn in solution (*46*−*48*), in keeping with this argument.

The mutagenesis of selected residues in the N-terminal domain of the β-subunit affected the binding of nucleotide or the catalysis of partial reaction 3 involving nucleotide, but not the binding of the other substrates or catalysis of partial reactions 1 and 2 involving succinyl-CoA and P_i. The positions of these mutated residues are shown as ball-and-stick models in Figure 2 and as asterisks in Figure 9. As demonstrated by the significant changes observed in the catalytic efficiency of the mutant proteins compared to that of the wild-type enzyme (Table 1), residues Gly 53β and Arg 54β are likely to be involved in the transfer of the γ-phosphate of nucleotide triphosphate to and from the active-site histidine, and the residue at position 20β has a role in determining the nucleotide specificity of SCS.

To further our understanding of the detailed interactions between nucleotide and SCS, analogue and substrate soaks of the native enzyme crystals are currently being carried out.

ACKNOWLEDGMENT

We thank Brian Tripet and Lorne Burke for their technical assistance during the mass spectrometry, Kim Oikawa (in the laboratory of Dr. Cyril Kay) for conducting circular dichroism analyses on the mutant proteins, and Jack Moore for performing the amino acid sequencing. We are grateful to Dr. Jean-Christophe Rochet for many insightful discussions and suggestions, and for reviewing the finished manuscript prior to submission.

REFERENCES

1. Bridger, W. A. (1974) in *The Enzymes* (Boyer, P. D., Ed.) 3rd ed., Vol. X, pp 581−606, Academic Press, New York.
2. Nishimura, J. S. (1986) in *Advances in Enzymology* (Meister, A., Ed.) Vol. 58, pp 141−172, Wiley, New York.
3. Ottaway, J. H., McClellan, J. A., and Saunderson, C. L. (1981) *Int. J. Biochem. 13*, 401−410.
4. Labbe, R. F., Kurumada, T., and Onisawa, J. (1965) *Biochim. Biophys. Acta 3*, 403−415.
5. Murakami, K., Mitchell, T., and Nishimura, J. S. (1972) *J. Biol. Chem. 247*, 6247−6252.
6. McClellan, J. A., and Ottaway, J. H. (1980) *Comp. Biochem. Physiol. 67B*, 679−684.
7. Hamilton, M. L., and Ottaway, J. H. (1981) *FEBS Lett. 123*, 252−254.
8. Jenkins, T. M., and Weitzman, P. D. J. (1988) *FEBS Lett. 230*, 6−8.
9. Bailey, D. L., Wolodko, W. T., and Bridger, W. A. (1993) *Protein Sci. 2*, 1255−1262.
10. Johnson, J. D., Mehus, J. G., Tews, K., Milavetz, B. I., and Lambeth, D. O. (1998) *J. Biol. Chem. 273*, 27580−27586.
11. Johnson, J. D., Muhonen, W. W., and Lambeth, D. O. (1998) *J. Biol. Chem. 273*, 27573−27579.
12. Lynn, R., and Guynn, R. W. (1978) *J. Biol. Chem. 253*, 2546−2553.
13. Jenkins, T. M., and Weitzman, P. D. J. (1986) *FEBS Lett. 205*, 215−218.
14. Pearson, P. H., and Bridger, W. A. (1975) *J. Biol. Chem. 250*, 8524−8529.
15. Wolodko, W. T., Fraser, M. E., James, M. N. G., and Bridger, W. A. (1994) *J. Biol. Chem. 269*, 10883−10890.
16. Murzin, A. G. (1996) *Curr. Opin. Struct. Biol. 6*, 386−394.
17. Fraser, M. E., James, M. N. G., Bridger, W. A., and Wolodko, W. T. (1999) *J. Mol. Biol. 285*, 1633−1653.
18. Kraulis, P. J. (1991) *J. Appl. Crystallogr. 24*, 946−950.
19. Collier, G. E., and Nishimura, J. S. (1978) *J. Biol. Chem. 253*, 4938−4943.
20. Mann, C. J., Hardies, S. C., and Nishimura, J. S. (1989) *J. Biol. Chem. 264*, 1457−1460.
21. Hara, T., Kato, H., Katsube, Y., and Oda, J. (1996) *Biochemistry 35*, 11967−11974.
22. Fan, C., Moews, P. C., Walsh, C. T., and Knox, J. R. (1994) *Science 266*, 439−443.
23. Wolodko, W. T., Kay, C. M., and Bridger, W. A. (1986) *Biochemistry 25*, 5420−5425.
24. Laemmli, U. K. (1970) *Nature 227*, 680.
25. Stanislawski, J. (1991) *ENZYME KINETICS*, version 1.11, Vol. 63, Trinity Software, Campton, NH.
26. Bridger, W. A., Ramaley, R. F., and Boyer, P. D. (1969) *Methods Enzymol. 13*, 70−75.
27. Norby, J., Rubenstein, S., Tuerke, T., Schwallie Farmer, C., Forood, R., and Bennington, J. (1993) *SIGMA PLOT*, version 4.11, Jandel Scientific, San Rafael, CA.
28. Hill, A. V. (1910) *J. Physiol. 40*, 4−7.
29. Jayaram, B., and Haley, B. E. (1994) *J. Biol. Chem. 269*, 3233−3242.
30. Ho, S. N., Hunt, H. D., Horton, R. N., Pullen, J. K., and Pease, L. R. (1989) *Gene 77*, 51−59.
31. Buck, D., and Guest, J. R. (1989) *Biochem. J. 260*, 737−747.
32. Sambrook, J., Fritsch, E. F., and Maniatis, T. (1989) *Molecular Cloning: a laboratory manual*, 2nd ed., Cold Spring Harbor Laboratory Press, Plainview, NY.
33. Davis, D. G., Dibner, M. D., and Battey, J. F. (1986) *Basic Methods in Molecular Biology*, 1st ed., Elsevier Science Publishing Co., Inc., New York.
34. Froehlich, B., and Epstein, W. (1981) *J. Bacteriol. 147*, 1117−1120.
35. Krebs, A., and Bridger, W. A. (1974) *Can. J. Biochem. 52*, 594−598.
36. Potter, R. L., and Haley, B. E. (1983) *Methods Enzymol. 91*, 613−633.
37. Moffet, F. J., Wang, T., and Bridger, W. A. (1972) *J. Biol. Chem. 247*, 8139−8144.
38. Buck, D., Spencer, M. E., and Guest, J. R. (1985) *Biochemistry 24*, 6245−6252.
39. Liang, T., and Schuster, G. B. (1987) *J. Am. Chem. Soc. 109*, 7803−7810.
40. King, S. M., Kim, H., and Haley, B. E. (1991) *Methods Enzymol. 196*, 449−466.
41. Vogel, H. J., and Bridger, W. A. (1983) *Biochem. Soc. Trans. 11*, 315−323.
42. Moffet, F. J., and Bridger, W. A. (1970) *J. Biol. Chem. 245*, 2758−2762.

43. Sweeny, J. R., and Fisher, J. R. (1968) *Biochemistry 7*, 561−565.
44. Westley, J. (1969) in *Enzymic Catalysis* (Halvorson, H. O., Roman, H. L., and Bell, E., Eds.) 1st ed., Harper and Row, New York.
45. Moffet, F. J., and Bridger, W. A. (1973) *Can. J. Biochem. 51*, 44−55.
46. Tavale, S. S., and Sobel, H. M. (1970) *J. Mol. Biol. 48*, 109−123.
47. Ikehara, M., Uesugi, S., and Yoshida, K. (1972) *Biochemistry 11*, 830−836.
48. Ikehara, M., Uesugi, S., and Yoshida, K. (1972) *Biochemistry 11*, 836−842.

BI990527S